

Multifragment emission in $^{36}\text{Ar}+^{197}\text{Au}$ and $^{129}\text{Xe}+^{197}\text{Au}$ collisions

W. Bauer, D.R. Bowman, N. Carlin^a, N. Colonna^b, R.T. de Souza^c, C.K. Gelbke, W.G. Gong, K. Hanold^b, Y.D. Kim, M.A. Lisa, W.G. Lynch, M.A. McMahan^b, L.G. Moretto^b, G.F. Peaslee, L. Phair, M.B. Tsang, C. Williams, G.J. Wozniak^b, and F. Zhu

NSCL, Michigan State University, East Lansing, MI 48824

^aUniversidade de São Paulo, C. Postal 20516, CEP 01498, São Paulo, Brazil

^bNuclear Science Division, Lawrence Berkeley Laboratory,
Berkeley, CA 94720

^cIUCF, Indiana University, Bloomington, IN 47405

Abstract

Multifragment disintegrations observed in $^{36}\text{Ar}+^{197}\text{Au}$ and $^{129}\text{Xe}+^{197}\text{Au}$ collisions are compared with theoretical predictions.

1. INTRODUCTION

Two phase transitions are expected to exist in bulk nuclear matter: a liquid-gas phase transition and a deconfinement transition to a quark-gluon plasma. Nuclear systems at densities and temperatures corresponding to the liquid-gas coexistence region are expected to decay into many intermediate mass fragments (IMF's: $Z=3-20$). We have studied multifragment exit channels for $^{36}\text{Ar}+^{197}\text{Au}$ collisions [1-4] at $E/A=35, 50, 80$, and 110 MeV and for $^{129}\text{Xe}+^{197}\text{Au}$ collisions at $E/A=50$ MeV [5] using the MSU Miniball [6].

2. RESULTS

The solid points in Fig. 1 show the average number of detected IMF's, $\langle N_{\text{IMF}} \rangle$, as a function of the raw charged particle multiplicity, N_c , for the Xe+Au reaction [5]. Calculations with the microscopic QMD and QPD models of refs. [7,8] predict average IMF multiplicities much smaller than observed experimentally. Both numerical simulations underestimate the growth of density fluctuations leading to fragment emission.

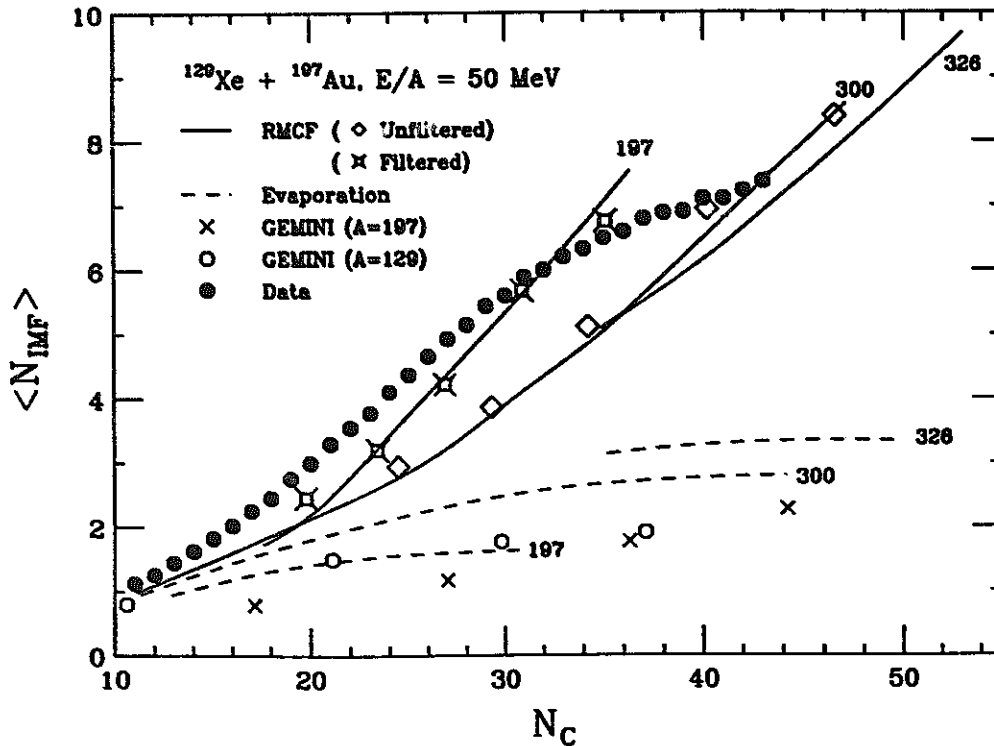


Fig. 1. Solid points: relation between $\langle N_{\text{IMF}} \rangle$ and N_C measured for Xe+Au reactions. Calculations are discussed in the text. Diamonds and star-shaped points illustrate instrumental distortions: Diamonds represent unfiltered distributions, star shaped points depict corresponding values filtered by the response of the experimental apparatus. From ref. [5].

Open circles and crosses in Fig. 1 show multiplicities predicted by the statistical code GEMINI [9]; dashed curves depict predictions of the statistical model of ref. [10]. These calculations for the decay of excited nuclei of normal nuclear density fail to reproduce the observed high IMF multiplicities. However, when hot nuclei are allowed to expand [11] significantly larger IMF multiplicities are predicted and reasonable agreement with the data is obtained (solid curves, star- and diamond-shaped points).

The solid points in Fig. 2 show the relationship between $\langle N_{\text{IMF}} \rangle$ and N_C observed [2,5] in Xe+Au and Ar+Au collisions at the indicated energies. Thick and thin curves represent results of filtered and unfiltered bond-percolation calculations [4,12], respectively, using the critical bond-breaking parameter, $p=0.7$. These calculations give upper bounds for the admixture of IMFs among the emitted charged particles. Solid and dashed curves show calculations for composite systems formed in Xe+Au and Ar+Au collisions; dot-dashed curves show calculations for the simultaneous multifragment decays of Xe projectile and Au target nuclei. The calculations are consistent with the IMF admixtures observed for the Ar+Au system, but they fail to reproduce the large values measured for the Xe+Au system.

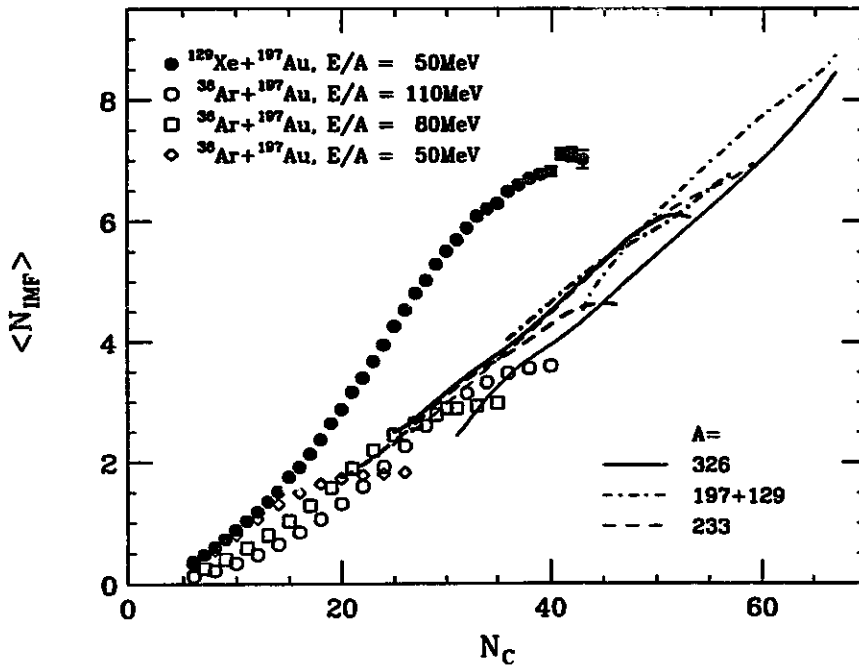


Fig. 2. Points show measured relation between $\langle N_{\text{IMF}} \rangle$ and N_c for the indicated reactions. Curves depict calculations with bond-percolation model [12] as explained in the text. From ref. [4].

The solid points in Fig. 3 show the relation between $\langle N_c \rangle$ and $\sigma_c^2 \langle N_c \rangle$ extracted for central Ar+Au collisions at $E/A=35, 50, 80,$ and 110 MeV. Here, $\langle N_c \rangle$ and σ_c^2 denote the mean value and the variance of the measured charged particle multiplicities. At all energies, the fluctuations of the charged particle multiplicity are considerably smaller than expected for Poisson distributions. This reduction of fluctuations in N_c may be caused by phase space constraints due to energy conservation. For example, calculations with the standard bond-percolation model do not incorporate effects related to energy conservation since the number of broken bonds is allowed to fluctuate; such calculations predict fluctuations in N_c (open circles) which are much larger than observed experimentally. If the effects of energy conservation are simulated by keeping the number of broken bonds fixed, the fluctuations are strongly reduced (open diamonds). Small fluctuations in N_c are also predicted by more realistic calculations performed with the microcanonical multifragmentation model [13] (star-shaped points) or the statistical code GEMINI [9] (square-shaped points) both of which incorporate energy conservation. The experimental N_c -distributions are somewhat broader than predicted by these latter two models, possibly due to imperfect impact parameter selection. Broadening due to poor impact parameter selection and implications for intermittency analyses are illustrated and discussed in ref. [4].

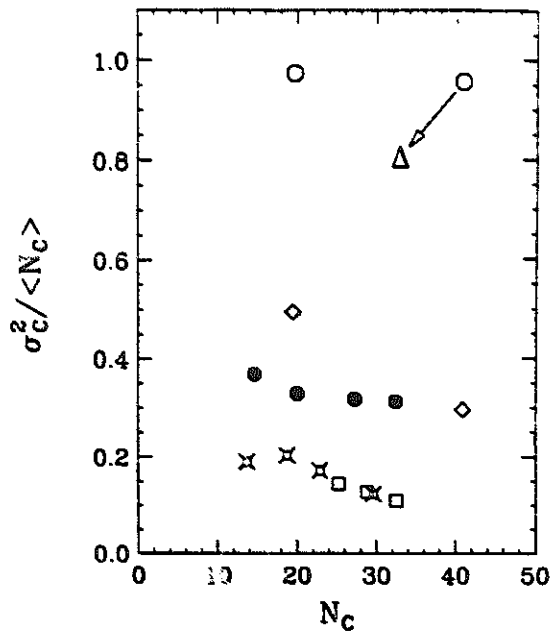


Fig. 3. Relation between $\sigma_c^2 / \langle N_c \rangle$ and $\langle N_c \rangle$. Solid points show experimental values extracted from near-central $^{36}\text{Ar}+^{197}\text{Au}$ reactions at $E/A=35, 50, 80$ and 110 MeV. Open points depict results of calculations. Open circles: standard bond-percolation model using $p=0.6$ and 0.7 (the open triangle illustrates the magnitude of instrumental distortions); open diamonds: percolation model with fixed number of broken bonds; open squares: predictions by GEMINI [9]; star-shaped points: predictions by Copenhagen fragmentation model [12]. From ref. [4].

3. REFERENCES

- 1 Y.D. Kim et al., Phys. Rev. Lett. 67 (1991) 14; Phys. Rev. C45 (1992)338; Phys. Rev. C45 (1992) 387.
- 2 R.T. de Souza et al., Phys. Lett. B268 (1991) 6.
- 3 M.B. Tsang et al., Phys. Rev. C44 (1991) 2065.
- 4 L. Phair et al., Phys. Lett. B and Nucl. Phys. A (in print).
- 5 D.R. Bowman et al., Phys. Rev. Lett. 67 (1991) 1527.
- 6 R.T. de Souza et al., Nucl. Instr. and Meth. A295 (1990) 109.
- 7 G. Peilert et al., Phys. Rev. C39 (1989) 1402.
- 8 D.H. Boal and J.N. Glosli, Phys. Rev. C37 (1988) 91; C42 (1990) R502.
- 9 R.J. Charity et al., Nucl. Phys. A483 (1988) 371.
- 10 W.A. Friedman and W.G. Lynch, Phys. Rev. C28 (1983) 16; C28 (1983) 950.
- 11 W.A. Friedman, Phys. Rev. C42 (1990) 667.
- 12 W. Bauer et al., Phys. Lett. 150B (1985) 53; Nucl. Phys. A452 (1986) 699; Phys. Rev. C38 (1988) 1927.
- 13 J.P. Bondorf et al., Nucl. Phys. A443 (1985) 321; Nucl. Phys. A444 (1986) 460; H.W. Barz, et al., Nucl. Phys. A448 (1986) 753.